Universality in fully developed turbulence

Siegfried Grossmann[1] and Detlef Lohse[1,2]
[1] *Fachbereich Physik, Philipps-Universität, Renthof 6, D-35032 Marburg, Germany*
[2] *The James Franck Institute, The University of Chicago, 5640 South Ellis Avenue, Chicago, Illinois 60637*
(Received 2 December 1993; revised manuscript received 27 April 1994)

We extend the numerical simulations of She *et al.* [Phys. Rev. Lett. **70**, 3251 (1993)] of highly turbulent flow with $15 \leq$ Taylor-Reynolds numbers $\mathrm{Re}_\lambda \leq 200$ up to $\mathrm{Re}_\lambda \approx 45\,000$, employing a reduced wave vector set method (introduced earlier) to approximately solve the Navier-Stokes equation. First, also for these extremely high Reynolds numbers Re_λ, the energy spectra as well as the higher moments—when scaled by the spectral intensity at the wave number k_p of peak dissipation—can be described by *one universal* function of k/k_p for all Re_λ. Second, the k-space inertial subrange scaling exponents ζ_m of this universal function are in agreement with the 1941 Kolmogorov theory (the better, the larger Re_λ is), as is the Re_λ dependence of k_p. Only around k_p, viscous damping leads to a slight energy pileup in the spectra, as in the experimental data (bottleneck phenomenon).

PACS number(s): 47.27.Gs, 47.11.+j, 47.27.Eq, 47.27.Jv

I. INTRODUCTION

A. Universal turbulent spectra

Very high Reynolds number turbulence still resists full numerical simulations. While in experiments Taylor-Reynolds numbers Re_λ up to $\mathrm{Re}_\lambda = 13\,000$ have been reported [1,2], the most turbulent *numerical* flow has—to our knowledge—been realized by She *et al.* [3], who achieve $\mathrm{Re}_\lambda = 200$ at a resolution of 512^3. These authors find that for all Re_λ up to $\mathrm{Re}_\lambda = 200$ all their energy spectra coincide when scaled by the spectral intensity at the wave number k_p of peak dissipation. That is, the function

$$\langle |\boldsymbol{u}(\boldsymbol{k})|^2 \rangle / \langle |\boldsymbol{u}(\boldsymbol{k}_p)|^2 \rangle = F^{(2)}(k/k_p) \qquad (1)$$

is universal as assumed by Kolmogorov and Obukhov [4]—both in the inertial subrange (ISR) and in the viscous subrange (VSR). Note that $F^{(2)}(1) = 1$ by definition. The universality is also found in experimental spectra [5]. For further numerical simulations, see also [6].

Kolmogorov and Obukhov [4] not only assumed universality of $F^{(2)}(k/k_p)$, but also its power law behavior $F^{(2)}(k/k_p) \propto (k/k_p)^{-\zeta_2}$ in the ISR with the classical exponent $\zeta_2 = 2/3$. (The scaling exponent 2/3 in the discrete Fourier transform, which we use here, corresponds to 5/3 in the continuous case.)

It has been argued in a long lasting debate (see, e.g., [7–9]) that there are small intermittency corrections to the classical scaling exponent $\zeta_2 = 2/3$. Unfortunately, even at today's state of the computational art [3], ζ_2 cannot sufficiently precisely be determined from full numerical simulations so that one could confirm or rule out deviations from 2/3. The reason is that for the tractable Re_λ the available wave number range is quite narrow ($k_p/k_{\min} \approx 5$ in [3]; $k_{\min}$ is the lowest wave number free of forcing). To obtain an ISR which extends over more than a decade, k_p must be larger than 50 $k_{\min}$ [3]. To realize this, a resolution $\geq 1500^3$ is required [3]. The required computer work increases as $\mathrm{Re}_\lambda^6 \log_2 \mathrm{Re}_\lambda$ [10]. We are thus far away from being able to create developed turbulence in a numerical flow for as high Re_λ as in experiment [1]. The huge gap between experiments and simulations is demonstrated in Table I. We therefore still need reasonable approximation techniques to numerically solve the Navier-Stokes equation.

B. Reduced wave vector set approximation for high Re turbulence

Such an approximation has been introduced by us in [11,12]. Meanwhile we could considerably improve our

TABLE I. In the first two lines Re, Re_λ, the length of the scaling range $k_p/k_{\min}$, and the number of contributing modes are compared for the most developed experimental and numerical turbulence, respectively. In the third line we give the same data for the largest Re of our reduced wave vector set approximation (REWA).

Method	Re	Re_λ	$k_p/k_{\min}$	No. of modes
best experiments [1,2]	1.7×10^8	13 000	$\approx 10\,000$	∞
best simulations [3]	$\approx 4 \times 10^4$	200	5	4×10^8
REWA [here]	1.4×10^7	45 000	$\approx 2\,000$	$80 \times 3 \times 13 = 3120$

approach [13]. Here we employ it to study universal features of fully developed turbulence for Reynolds numbers Re between 730 and 1.4×10^7 (corresponding to Taylor-Reynolds numbers Re_λ between 120 and 45 000, see Table II below). This leads to remarkably large ISR's. For Re= 1.4×10^7, the extension of the ISR is $k_p/k_{\min} \approx 2000$, i.e., more than three decades, compared to $k_p/k_{\min} \approx 5$ achieved in the presently best Navier-Stokes simulation [3].

For completeness we briefly repeat the main idea of our approximation. To deal feasibly with the many scales present in turbulent flow, we only admit a geometrically scaling subset K of wave vectors in the Fourier sum, $K = \cup_l K_l$, thus $u_i(\boldsymbol{x},t) = \sum_{\boldsymbol{k}\in K} u_i(\boldsymbol{k},t)\exp(i\boldsymbol{k}\cdot\boldsymbol{x})$. $K_0 = \{\boldsymbol{k}_n^{(0)},\ n = 1,...,n_{\max} = 80\}$ contains appropriately chosen wave vectors, $K_l = \{\boldsymbol{k}_n^{(l)} = 2^l\boldsymbol{k}_n^{(0)},\ n = 1,...,n_{\max} = 80\}$, $l = 1,...,l_{\max}$, which are a scaled replica of K_0. The degree of nonlocality of the approximate Navier-Stokes interaction is determined by the choice of K_0. Here we consider triad interactions with a ratio up to ≈ 5 between the largest and the smallest wave vector, but extended calculations [14] (up to a ratio between ≈ 6 and ≈ 11) show that our conclusions do not depend on that ratio. The choice of $l_{\max}$ depends on the control parameter ν, the viscosity. The incompressible Navier-Stokes equation is solved on K with periodic boundary conditions in a box of size $(2\pi L)^3$. All lengths will from now on be measured in multiples of L, so the smallest component of the smallest wave vector is 1. The flow is permanently, nonstochastically forced on the outer length scale with energy input rate ϵ. All times will henceforth be given in multiples of $(L^2/\epsilon)^{1/3}$, i.e., the energy input and thus in the stationary case also the energy dissipation rate is $\epsilon = 1$. The type of forcing does not influence our results sizably [13]. The smallest wave vectors whose amplitudes are free of forcing have length $k_{\min} = 3$. The smallest wave vectors at all are $\pm(1,1,-2)$ plus permutations and thus have length $\sqrt{6} = 0.82k_{\min}$. All wave vector amplitudes $\boldsymbol{u}(\boldsymbol{k},t)$ with $|\boldsymbol{k}| \geq k_{\min} = 3$ are free of forcing.

C. Contents of the paper and summary

The paper is organized as follows. In Sec. II we examine the Re dependence of the Taylor-Reynolds number. In Sec. III we confirm universality up to the highest Re= 1.4×10^7 we can treat, which is our main result. The form of the universal spectra is discussed in Sec. IV. Hardly any nonclassical scaling corrections are found in the middle of the k-space inertial subrange, but intermittency shows up in the stirring subrange and in the viscous subrange. Near peak dissipation k_p there is an energy pileup due to a viscosity induced bottleneck phenomenon [15,16].

II. Re DEPENDENCES

What are the Reynolds numbers Re of our approximate numerical turbulence? As usual, there is some arbitrariness in the definition of the Reynolds number. We regard $L_0 = \lambda/2$ as the outer length scale, where λ is the wavelength of the smallest wave vector, and $U_0 = 2u_{1,\mathrm{rms}}$ is the typical velocity difference on the outer length scale. Thus Re= U_0L_0/ν can be considered as an appropriate definition of the Reynolds number. The data for five simulations, covering four decades of Re, are given in Table II. We also list the Taylor-Reynolds numbers $\mathrm{Re}_\lambda = u_{1,\mathrm{rms}}\lambda_{\mathrm{Taylor}}/\nu$, where $\lambda_{\mathrm{Taylor}} = u_{1,\mathrm{rms}}/(\partial_1 u_1)_{\mathrm{rms}}$ are the Taylor lengths.

The dissipation rate is balanced by the input rate $\epsilon \sim U_0^3/L_0$ [17,18]. We therefore write

$$\epsilon = c_\epsilon U_0^3/L_0, \tag{2}$$

where c_ϵ is a dimensionless number. Since we choose $\epsilon = 1$, $L_0 = \pi/\sqrt{6}$, and since we find $U_0 = 2u_{1,\mathrm{rms}}$ from the numerical solution, we can determine c_ϵ from this equation. It turns out to decrease with increasing Re, seemingly to a final level somewhere near 6×10^{-3}. Note that for laminar flow, on the other hand, it holds $c_\epsilon \propto \mathrm{Re}-1$, see, e.g., [17].

Equation (2) leads to the relation

$$\mathrm{Re}_\lambda = \sqrt{\frac{15}{16c_\epsilon}}\sqrt{\mathrm{Re}}. \tag{3}$$

When c_ϵ eventually becomes universal, i.e., independent of Re, the well known large Re limit relation $\mathrm{Re}_\lambda \propto \sqrt{\mathrm{Re}}$ is recovered. In experiment, for smaller Re the measured Taylor-Reynolds number Re_λ turns out to be smaller

TABLE II. Results from our approximate solutions of the Navier-Stokes equation for various ν. $l_{\max}+1$ is the number of rescaled wave number replica K_l. The definition of Re is Re= U_0L_0/ν. Here $L_0 = \pi/\sqrt{6}$, and $U_0 = 2u_{1,\mathrm{rms}}$ describes the velocity difference across the outer scale, being determined for each ν from our numerical solution. ($u_{1,\mathrm{rms}}$ depends on ν and increases from 1.42 to 2.73 for the ν in the table.) $\mathrm{Re}_\lambda = u_{1,\mathrm{rms}}\lambda_{\mathrm{Taylor}}/\nu$, as usual. The coefficient c_ϵ is calculated according to Eq. (2). In the last two columns the extension of the scaling range, $\log_{10}(k_p/k_{\min})$ (found from the numerical solution), is compared with that calculated from Eq. (4′), see text.

ν	$l_{max}+1$	Re	Re_λ	$c_\epsilon(\mathrm{Re})$	$\log_{10}(k_p/k_{\min})$	$\log_{10}(c_\eta \mathrm{Re}^{3/4})$
5×10^{-3}	5	730	122	46×10^{-3}	0.24	0.08
5×10^{-4}	7	1.05×10^4	801	15×10^{-3}	0.97	0.95
5×10^{-5}	9	1.25×10^5	3 590	9.1×10^{-3}	1.79	1.75
5×10^{-6}	11	1.37×10^6	13 600	7.0×10^{-3}	2.48	2.53
5×10^{-7}	13	1.40×10^7	44 800	6.5×10^{-3}	3.29	3.29

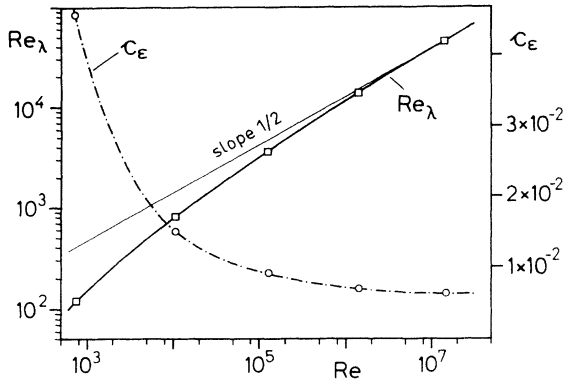

FIG. 1. Re$_\lambda$ (squares) and c_ϵ (circles) as functions of Re. Left ordinate is Re$_\lambda$, right ordinate is c_ϵ. For large Re the power law Re$_\lambda \propto \sqrt{\text{Re}}$ holds, for small Re there are deviations, as the dimensionless number c_ϵ in Eq. (2) depends on Re. The dependence of c_ϵ on Re strongly resembles the experimental one, cf. [19,22,17].

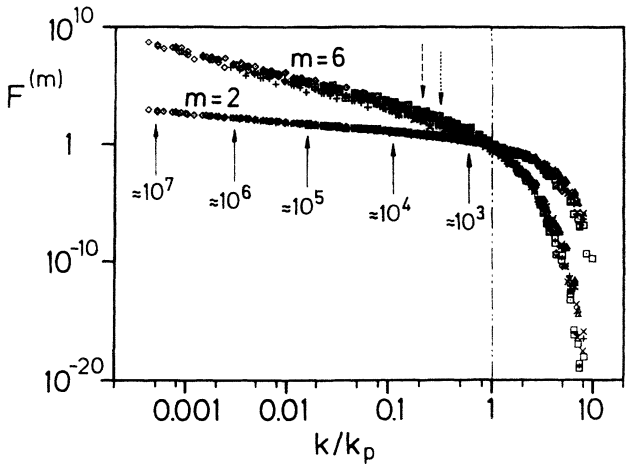

FIG. 2. Universal spectra $F^{(m)}(k/k_p)$ for $m = 2$ (flatter) and $m = 6$ (steeper) for Re $= 7.3 \times 10^2$ (triangles), Re $= 1.05 \times 10^4$ (crosses), Re $= 1.25 \times 10^5$ (squares), Re $= 1.37 \times 10^6$ (pluses), Re $= 1.40 \times 10^7$ (diamonds). The arrows indicate the smallest wave number *free of forcing*, $k_{\min}$, for the respective Re. The smallest wave number *of all* $\boldsymbol{k} \in K$ is $0.82k_{\min}$, see Sec. I B. The dashed arrow labels $k_{\min}$ in the simulation by She *et al.* [3], the dotted arrow marks $k_{\min}$ in the one of Vincent and Meneguzzi [6].

than predicted by Re$_\lambda \propto \sqrt{\text{Re}}$ [19,20], as in fact c_ϵ depends on Re. Both the large Re behavior of Re$_\lambda$ with the power law exponent 1/2 and the deviations for smaller Re can also be seen in our approximate solutions, see Fig. 1. For a more detailed discussion on the Re dependence of c_ϵ and Re$_\lambda$, see [21,22].

One remark concerning the nominal value of the prefactor in Eq. (3). Taking the large Reynolds numbers, we have (with $c_\epsilon = 6.5 \times 10^{-3}$ from Table II) Re$_\lambda \approx 12\sqrt{\text{Re}}$, whereas experimentally it is Re$_\lambda \sim \sqrt{\text{Re}}$, i.e., we overestimate the Taylor-Reynolds numbers by one order of magnitude. We explain this as due to our approximation, as in our reduced wave vector set K the larger wave vectors are considerably thinned out. So less energy than ought to be is transported downscale, leading to a larger $u_{1,\text{rms}}$ than in real turbulence and thus to a larger Re$_\lambda = u_{1,\text{rms}}^2/\nu(\partial_1 u_1)_{\text{rms}}$. The same blocking effect by phase space sparseness at larger k also leads to an overestimation of the Kolmogorov constant b in the velocity structure function $D(r) = b(\epsilon r)^{2/3}$ as already mentioned in [13,12] — also by a factor of about 10 ($b \approx 70$ instead of $b = 8.4$ as in experiment, see [13]), because both Re$_\lambda$ and $D(r)$ are quadratic in $u_{1,\text{rms}}$. [Note that the denominator $(\partial_1 u_1)_{\text{rms}}$ is proportional to $\sqrt{\epsilon}$ and thus kept fixed.]

III. UNIVERSAL WAVE NUMBER SPECTRA

The wave number spectra of our approximate solutions are shown in Fig. 2, which constitutes our main result. We can confirm that $F^{(2)}(k/k_p)$ in fact is *universal* for all Re even much beyond Re$_\lambda = 200$ as studied in [3]. In particular we hint at the remarkable universality also in the VSR. As in [3], the wave number k_p of peak dissipation is found to increase as $\text{Re}^{3/4}$, i.e., ηk_p is constant also for the huge Re we simulated, see Table III. We find $k_p \approx 1/10\eta$. For Re$= 1.4 \times 10^7$ the ISR extends as far as 3.3 decades to the left of k_p, see Table II. In k space $\log_{10}(k_p/k_{\min})$ gives the extension of the ISR. This extension of the scaling range should also follow from the Reynolds number Re. In r space the scaling occurs between the outer length scale L_0 and 10η, where $\eta = \nu^{3/4}/\epsilon^{1/4}$ is the Kolmogorov length scale [17,18]. For large Re it is [17]

$$L_0/10\eta = c'_\eta \text{Re}^{3/4}. \tag{4}$$

Formally Eq. (4) can be derived from Eq. (2) and one gets $c'_\eta = c_\epsilon^{1/4}/10$. Note that thus c'_η is also slightly Re dependent via c_ϵ(Re). Yet our c_ϵ is smaller than the experimental one, see last paragraph of Sec. II. Therefore we rather define a c_η from the extension of the scaling range found in our numerical simulation than from (4), namely, by

$$k_p/k_{\min} = c_\eta \text{Re}^{3/4}. \tag{4'}$$

This corresponds to (4) since L_0 is approximately $1/k_{\min}$ and 10η is approximately $1/k_p$. More precisely we have $L_0 = 3\pi/(\sqrt{6}\,k_{\min})$, so $L_0^{-1} = 0.26\,k_{\min}$. The ratio $k_p/k_{\min}$ can be extracted from our numerical spectra in k space. For the largest Re$= 1.4 \times 10^7$ we find $k_p/k_{\min} = 1950$ and thus obtain $c_\eta = (k_p/k_{\min})\text{Re}^{-3/4} = 8.52 \times 10^{-3}$. We now disregard the small Re dependence of c_η and calculate the extension of the scaling ranges for smaller Re from (4′) with $c_\eta = 8.52 \times 10^{-3}$. The results are given in the last column of Table II and are found in excellent agreement with the length of the scaling ranges seen in our approximate solutions for these smaller Re, see sixth column of Table II. We find disagreement only for the smallest Re, as expected, because for Re=730 the constant c_η in Eq. (4′) can no longer be considered as independent of Re.

Moreover, the $F^{(m)}(k/k_p) = \langle|\boldsymbol{u}(\boldsymbol{k})|^m\rangle/\langle|\boldsymbol{u}(\boldsymbol{k}_p)|^m\rangle$, m=3,4,6,8,10, are also found to be *universal* (see Fig. 2 for $m = 6$). Due to the very extended ISR we can

TABLE III. The fit parameters to our approximate solutions of the Navier-Stokes equation for the same ν as in Table II. k_p is the wave number with peak dissipation, $k_d^{(2)}$ the cutoff from our fit (5), if we fit the spectrum in the interval $[0,\eta^{-1}/4]$. In the last column their ratio $\tilde{k}_d^{(2)} = k_d^{(2)}/k_p$ is given. From the condition $\tilde{k}^2 F^{(2)}(\tilde{k})$ maximal at 1, the cutoff should be $\tilde{k}_d^{(2)} = 3/4$.

ν	ζ_2	ζ_6	$(k_p\eta)^{-1}$	$(k_d^{(2)}\eta)^{-1}$	$\tilde{k}_d^{(2)}$
5×10^{-3}	0.656	1.997	10.2	11.8	0.87
5×10^{-4}	0.678	1.986	10.6	13.6	0.78
5×10^{-5}	0.672	1.975	9.2	13.7	0.67
5×10^{-6}	0.669	1.994	10.5	13.3	0.79
5×10^{-7}	0.668	1.990	9.1	13.3	0.67

determine the power law exponents ζ_m of the universal functions $F^{(m)}(k/k_p) \propto (k/k_p)^{-\zeta_m}$ rather precisely, cf. Table III. This is still not possible in full simulations, as the universal scaling range is too small, $k_p/k_{\min} \leq 5$ [6,3]. If a power law fit for full simulations is tried nevertheless, one gets scaling exponents ζ_m much smaller than the classical ones, due to the nonuniversal large scale forcing [6,23] and the bottleneck phenomenon [15,16]. E.g., $\xi_2 \approx 0.57$ is found in [6], which can be accounted for in [16].

IV. FORM OF THE UNIVERSAL SPECTRA

Having shown universality, we now check several fits to the universal spectra $F^{(m)}(k/k_p)$ that we obtained from our numerical data.

A. Scaling exponents in k space

The simplest way to determine scaling exponents is to fit the spectra for all Re by the two parameter function

$$F^{(m)}(\tilde{k}) = \tilde{k}^{-\zeta_m}\exp[-(\tilde{k}-1)/\tilde{k}_d^{(m)}],$$
$$\tilde{k} = k/k_p, \qquad (5)$$
$$\tilde{k}_d^{(m)} = k_d^{(m)}/k_p.$$

This form has theoretical support [24] and was also successfully used to fit experimental spectra [25,26]. The crossover between the power law behavior in the ISR and exponential fall off in the VSR takes place at the wave number $k_d^{(m)}$. In Table III we list the parameters, obtained from a fit in the range $0 \leq k \leq \eta^{-1}/4$ or $0 \leq k/k_p \leq 2.5$, respectively. The fit (5) gives ζ_3 rather near, but not exactly equal to 1 as it should be according to Kolmogorov's structure equation [18]. This tiny deviation is corrected in Table III by dividing the scaling exponents obtained from the fit (5) by ζ_3. The resulting scaling exponents take their classical values $\zeta_m = m/3$ with high accuracy, see Table III.

From the appearance of the classical scaling exponents $\zeta_m = m/3$ one might deduce that there is no intermittency in our signal. This conclusion would not be correct. In fact, for small scales we do observe strong intermittency in the signal [11,13]. We therefore suggested introduction of local $\zeta_m(k)$, defined by local fits of type (5) in the restricted k ranges $[k/\sqrt{10}, k\sqrt{10}]$ for all k, keeping the $k_d^{(m)}$ fixed at their global values [13].

The surprising result is shown in Fig. 3. There are large intermittency corrections $\delta\zeta_m(k) = \zeta_m(k) - m/3$ at small scales (VSR), only moderate intermittency corrections at large scales [stirring subrange (SSR)], but hardly any deviations from classical scaling in the ISR. This astonishing result was extensively discussed already in [13]. Here it can be confirmed for a considerably larger Re range.

In addition, we fitted Eq. (5) to our spectra, but now with $k_d^{(m)}$ *fixed* at $k_d^{(m)} = 2k_d^{(2)}/m$, $k_d^{(2)} = (13.5\eta)^{-1}$, see below. Again we find only tiny global intermittency corrections, which clearly *decrease* with increasing Re, as predicted by [19,27]. For Re$= 1.05\times10^4$ we find $\delta\zeta_2 = 0.012$, $\delta\zeta_6 = -0.058$, going down to $\delta\zeta_2 = 0.002$, $\delta\zeta_6 = -0.011$ for Re$= 1.4\times10^7$, suggesting that intermittency might be a finite size effect. For details and a theoretical explanation we refer to Ref. [28].

When comparing our scaling exponents to experimental ones, one should note that all scaling exponents determined in this paper refer to *k-space* moments, as our method clearly is a wave vector space method. In principle we can calculate the complete r space velocity field by performing the Fourier transformation on the reduced wave vector set K. But due to the sparseness of K at larger k the small r-space structures will be underestimated and the scaling of velocity structure functions is less pronounced in r space than in k space [11,14]. Recent calculations [29] show that scaling corrections can be quite different in r versus k space. So the measured anomalous scaling exponents of r-space velocity structure functions [8,30–32] do not contradict our k-space results, in particular, as the experiments are performed at relatively low Reynolds number $\mathrm{Re}_\lambda \leq 2720$ [8,30] or Re$<$ 300 000 [32]. On the other hand, recent k-space measurements [2] (or rather velocity power spectra obtained by Taylor's hypothesis which we do not want to discuss here) for very high $\mathrm{Re}_\lambda = 12\,700$ did not show any detectable deviation from classical scaling. For Re$\to\infty$, of course, k- and r-space scaling exponents should agree.

We now discuss the crossover scale between ISR and VSR. From the fit (5) we get $(k_d^{(2)})^{-1} \approx 13.5\eta$, i.e., the crossover scale is one order of magnitude larger than

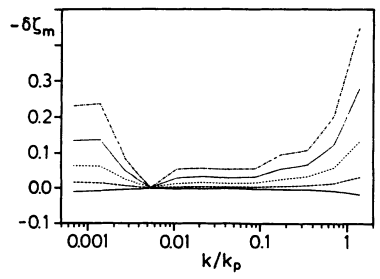

FIG. 3. Scale resolved intermittency corrections $-\delta\zeta_m(k)$ for $m = 2,4,6,8,10$, bottom to top. $\nu = 5\times10^{-7}$, Re $= 1.4\times10^7$. The fit range is $[k/\sqrt{10}, k\sqrt{10}]$ for all k.

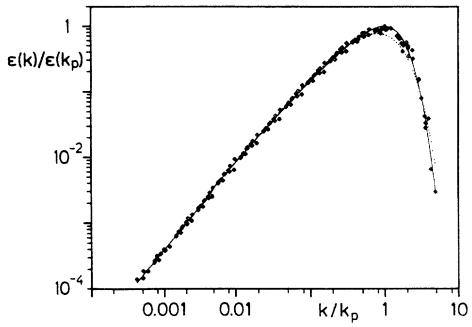

FIG. 4. Universal energy dissipation rate $\epsilon(k)/\epsilon(k_p)$ versus k/k_p for $\nu = 5 \times 10^{-7}$, Re $= 1.4 \times 10^7$. Also shown are the fits resulting from (5) (dashed) and (6) (solid).

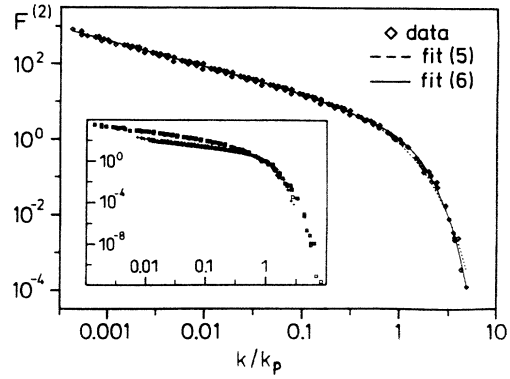

FIG. 5. Universal spectrum $F^{(2)}(k/k_p)$ for $\nu = 5 \times 10^{-7}$, Re $= 1.4 \times 10^7$. The fits (5) (dashed) and (6) (solid) are compared, both with the same $\zeta_2 = 2/3$. Inset: Quality of universality in the log-similarity description for the second moments, see text. The symbols mean Re $= 1.25 \times 10^5$ (squares), Re $= 1.37 \times 10^6$ (pluses), Re $= 1.40 \times 10^7$ (diamonds). On the abscissa we plotted $\beta \log_{10}[k/(2k_p)]$, on the ordinate $\beta \log_{10}[\langle|\boldsymbol{u}(k)|^2\rangle/\langle|\boldsymbol{u}(2k_p)|^2\rangle]$ with $\beta = 0.9/\log_{10}(\mathrm{Re}_\lambda/75)$, cf. [19].

the Kolmogorov length. This fact has long been known from experiment [18] and theory [33]. From the maximum condition for $k^2F^{(2)}(k)$ at $k = k_p$ it follows that $\tilde{k}_d^{(2)} = 1/(2 - \zeta_2) = 3/4$. In our simulations there are some fluctuations around this value. The reason is that we have *discrete* wave vectors which are not dense in the VSR. Thus k_p can only be determined with limited accuracy, cf. Fig. 4, where the energy dissipation rate $\epsilon(k) = \boldsymbol{k}^2\langle|\boldsymbol{u}(\boldsymbol{k})|^2\rangle$ is displayed. Typically the relative k distances are $\delta k/k \approx 1/10$, which corresponds to the $\approx 10\%$ deviations of $\tilde{k}_d^{(2)}$ from 0.75 in Table III. Of course, to increase the accuracy of k_p, one could also define it in terms of $k_d^{(2)}$ from the global fit (5) with fixed $\zeta_2 = 2/3$ to be $k_p = 4k_d^{(2)}/3$. The resulting small changes are not visible in Fig. 2.

Where does the crossover from ISR to VSR behavior take place in higher order moments? From the fit (5) we find $k_d^{(m)} = 2k_d^{(2)}/m$, i.e., $\tilde{k}_d^{(m)} = 3/(2m)$ to a very high precision [13]. This means that the ISR is considerably *smaller* for higher order moments, or, to state it differently, higher order moments are affected by viscosity earlier than lower order moments.

B. Energy pileup in the crossover region between ISR and VSR

We also applied fits different from (5), as from Fig. 5 it might seem that (5) only badly fits the spectrum in the range around k_p. The same observation was reported already by She and Jackson [5] when they determined the universal function $F^{(2)}(k/k_p)$ from experimental data. To improve the fit, they suggested use of the empirical three parameter function

$$F^{(2)}(\tilde{k}) = \frac{\tilde{k}^{-2/3}}{1+\alpha}(1 + \alpha\tilde{k}^{\beta}) \exp[-(\tilde{k} - 1)/\tilde{k}_d^{(2)\prime}],$$
$$\tilde{k} = k/k_p, \qquad (6)$$
$$\tilde{k}_d^{(2)\prime} = k_d^{(2)\prime}/k_p,$$

and found $\alpha = 0.8$, $\beta \approx 0.7$, i.e., near $k = k_p$ the decay of the spectral power is diminished. Their physical interpretation is a pileup of excitation around k_p, possibly due to coherent vortex structures. Note that Eq. (6) results in a nonmonotonous local slope $d\ln F(k)/d\ln k$.

We also tried the fit (6) and found $\alpha \approx 2$, $\beta \approx 1.8$, and $\tilde{k}_d^{(2)\prime} \approx 0.4$, all slightly depending on Re. Thus the energy pileup at $k \approx k_p$ in our approximate Navier-Stokes solution seems to be even stronger than in the experiment [5], as we have an additive correction term with a *larger* exponent. Of course, $F^{(2)}(k/k_p)$ does not increase with k/k_p as the correction term is strongly damped by $\exp(-k/k_d^{(2)\prime})$ with $k_d^{(2)\prime}$ much smaller as $k_d^{(2)}$ before. The energy pileup can also be observed in Fig. 5, where we replotted $F^{(2)}(k/k_p)$ with the two fits Eq. (5), where we fixed $\zeta_2 = 2/3$, and Eq. (6). For $k \approx k_p$ the fit (6) is slightly superior to the fit (5).

The energy pileup, according to Falkovich [15], may be explained by the so called bottleneck phenomenon [15]. This phenomenon can be described as follows. Imagine a triad Navier-Stokes interaction between the amplitudes $\boldsymbol{u}(\boldsymbol{k}_1)$, $\boldsymbol{u}(\boldsymbol{k}_2)$, and $\boldsymbol{u}(\boldsymbol{k}_3)$, $\boldsymbol{k}_1 + \boldsymbol{k}_2 + \boldsymbol{k}_3 = 0$, $k_1 < k_{2,3}$, so that $\boldsymbol{u}(\boldsymbol{k}_2)$ and $\boldsymbol{u}(\boldsymbol{k}_3)$ are already considerably damped by viscosity, in additon to the power law decrease $\propto k^{-2/3}$. So the turbulent energy transfer downscale $\sim k_1 u(k_1) u(k_2) u(k_3)$ would be reduced and stationarity could not be achieved, if $\boldsymbol{u}(\boldsymbol{k}_1)$ did not increase, i.e., an energy pileup at k_1 is established. The effect is strongest if k_1 is around k_p, because there $\boldsymbol{u}(\boldsymbol{k}_2)$ and $\boldsymbol{u}(\boldsymbol{k}_3)$ are already considerably damped. Of course, there is also viscous damping around k_1, which would counteract the bottleneck effect, but for $k_1 < \eta^{-1}$ the damping by viscosity ν is weaker than the damping by the *eddy* viscosity [15].

In Ref. [16] the bottleneck phenomenon has been connected with the relatively sharp crossover from VSR to ISR in the r-space velocity structure function $D(r)$. The numerical and experimental $D(r)$ [32] with a

monotonously decreasing local slope $d\ln D(r)/d\ln r$ lead to spectra of type (6) with $\alpha \approx 2.6$, $\beta = 2$, very near to our above result [16].

The same pileup as for $F^{(2)}(k)$ also appears in higher order velocity moments $\langle |\boldsymbol{u}(\boldsymbol{k})|^m \rangle$ with $m > 2$, leading to smaller local scaling exponents $\zeta_m(k)$ for k near the VSR. Possibly this effect mimics intermittency corrections to classical scaling in experimental data or simulated data with shorter scaling ranges which in fact would not show up in sufficiently long ISR for large enough Re. This interpretation is also supported by the behavior of the scale resolved intermittency exponents, $\zeta_m(k)$, see Fig. 3 above and Ref. [13].

C. Log-similarity description of the spectra

Finally, besides the normalization of the spectra (1) another procedure has been suggested to get a universal description of the experimental data, namely, the log-similarity description [19]. This claims that the logarithmic spectra coincide for different Re_λ, when both the abscissa and the ordinate are multiplied by some function $\beta(\mathrm{Re}_\lambda)$, i.e., $\beta \log_{10}[|\boldsymbol{u}(\boldsymbol{k})|^2/|\boldsymbol{u}(\boldsymbol{k}_0)|^2]$ against $\beta \log_{10}(k/k_0)$ is claimed to be universal. k_0 is a wave number which has to be fitted to the experimental data. In [19] $k_0 \approx 2k_p \approx (6\eta)^{-1}$ is found. For large Re_λ it is $\beta = 0.9/\log_{10}(\mathrm{Re}_\lambda/75)$ [19]. We plot the spectra for our three largest Re in this parametrization, see inset of Fig. 5. As Taylor-Reynolds number we simply take $\sqrt{\mathrm{Re}}$, because our approximation overestimates Re_λ, see the discussion in Sec. II. For smaller Re the function $\beta(\mathrm{Re}_\lambda)$ behaves quite differently, so it is not reasonable to show also the spectra for smaller Re in the plot. The quality of the superposition of the spectra might improve if one readjusted the free parameters of this description.

ACKNOWLEDGMENTS

We are grateful to B. Castaing, G. Falkovich, Th. Gebhardt, L. Kadanoff, and A. Reeh for very helpful discussions. D. L. thanks the Aspen Center of Physics for its hospitality. Partial support by the German-Israel Foundation (GIF), by DOE, and by a NATO grant through the Deutsche Akademische Austauschdienst (DAAD) is gratefully acknowledged. The HLRZ Jülich supplied us with computer time.

[1] H. L. Grant, R. W. Stewart, and A. Moilliet, J. Fluid Mech. **12**, 241 (1961); A. L. Kistler and T. Vrebalovich, *ibid.* **26**, 37 (1966); R. W. Williams and C. A. Paulson, *ibid.* **83**, 547 (1977); F. H. Champagne, *ibid.* **86**, 67 (1978).
[2] A. Praskovsky and S. Oncley, Phys. Fluids A **6**, 2886 (1994).
[3] Z. S. She, S. Chen, G. Doolen, R. H. Kraichnan, and S. A. Orszag, Phys. Rev. Lett. **70**, 3251 (1993).
[4] A. N. Kolmogorov, C. R. (Dokl.) Acad. Sci. URSS **30**, 299 (1941); A. M. Obukhov, *ibid.* **32**, 19 (1941).
[5] Z. S. She and E. Jackson, Phys. Fluids A **5**, 1526 (1993).
[6] R. Kerr, J. Fluid Mech. **153**, 31 (1985); **211**, 309 (1990); A. Vincent and M. Meneguzzi, *ibid.* **225**, 1 (1991).
[7] A. N. Kolmogorov, J. Fluid Mech. **13**, 82 (1962).
[8] F. Anselmet, Y. Gagne, E. J. Hopfinger, and R. Antonia, J. Fluid Mech. **140**, 63 (1984).
[9] C. Meneveau and K. R. Sreenivasan, J. Fluid Mech. **224**, 429 (1991).
[10] S. A. Orszag, J. Fluid Mech. **41**, 363 (1970).
[11] S. Grossmann and D. Lohse, Z. Phys. B **89**, 11 (1992); Physica A **194**, 519 (1993).
[12] J. Eggers and S. Grossmann, Phys. Fluids A **3**, 1958 (1991).
[13] S. Grossmann and D. Lohse, Phys. Fluids **6**, 611 (1994); Phys. Scr. **T49**, 77 (1993).
[14] S. Grossmann, D. Lohse, and A. Rech, in *Proceedings of the International Conference on Dynamical Systems and Chaos*, edited by S. Saito (World Scientific, Singapore, in press).
[15] G. Falkovich, Phys. Fluids **6**, 1411 (1994).
[16] D. Lohse and A. Müller-Groeling (unpublished).
[17] L. D. Landau and E. M. Lifshitz, *Fluid Mechanics* (Pergamon Press, Oxford, 1987).
[18] A. S. Monin and A. M. Yaglom, *Statistical Fluid Mechanics* (MIT Press, Cambridge, MA, 1975).
[19] B. Castaing, Y. Gagne, and M. Marchand, Physica D **68**, 387 (1993).
[20] D. P. Lathrop, Jay Fineberg, and H. S. Swinney, Phys. Rev. Lett. **68**, 1515 (1992); C. Doering and P. Constantin, *ibid.* **69**, 1648 (1992).
[21] D. Lohse (unpublished); C. Doering and P. Constantin, Phys. Rev. E **49**, 4087 (1994).
[22] K. R. Sreenivasan, Phys. Fluids **27**, 1048 (1984).
[23] R. Kerr (private communication).
[24] C. Foias, O. Manley, and L. Sirovich, Phys. Fluids A **2**, 464 (1990).
[25] K. R. Sreenivasan, J. Fluid Mech. **151**, 81 (1985).
[26] I. Procaccia, E. S. C. Ching, P. Constantin, L. P. Kadanoff, A. Libchaber, and X. Z. Wu, Phys. Rev. A **44**, 8091 (1991).
[27] V. S. L'vov and I. Procaccia, Phys. Rev. E **49**, 4044 (1994).
[28] S. Grossmann, D. Lohse, V. L'vov, and I. Procaccia, Phys. Rev. Lett. **73**, 432 (1994).
[29] D. Lohse and A. Müller-Groeling (unpublished).
[30] B. Castaing, Y. Gagne, and E. J. Hopfinger, Physica D **46**, 177 (1990).
[31] R. Benzi, S. Ciliberto, R. Tripiccione, C. Baudet, F. Massaioli, and S. Succi, Phys. Rev. A **48**, 29 (1993).
[32] R. Benzi, S. Ciliberto, C. Baudet, and G. R. Chavarria (unpublished).
[33] H. Effinger and S. Grossmann, Z. Phys. B **66**, 289 (1987).